Brief Report

Epsin 1 Undergoes Nucleocytosolic Shuttling and its Eps15 Interactor NH$_2$-terminal Homology (ENTH) Domain, Structurally Similar to *Armadillo* and HEAT Repeats, Interacts with the Transcription Factor Promyelocytic Leukemia Zn^{2+} Finger Protein (PLZF)

Joel Hyman,*§ Hong Chen,‡§ Pier Paolo Di Fiore,‖ Pietro De Camilli,‡§ and Axel T. Brunger*§

*Department of Molecular Biophysics and Biochemistry, ‡Department of Cell Biology, and §Howard Hughes Medical Institute, Yale University, New Haven, Connecticut 06520; and ‖Department of Experimental Oncology, European Institute of Oncology, Milan, Italy.

Abstract. Epsin (Eps15 interactor) is a cytosolic protein involved in clathrin-mediated endocytosis via its direct interactions with clathrin, the clathrin adaptor AP-2, and Eps15. The NH$_2$-terminal portion of epsin contains a phylogenetically conserved module of unknown function, known as the ENTH domain (epsin NH$_2$-terminal homology domain). We have now solved the crystal structure of rat epsin 1 ENTH domain to 1.8 Å resolution. This domain is structurally similar to *armadillo* and Heat repeats of β-catenin and karyopherin-β, respectively. We have also identified and characterized the interaction of epsin 1, via the ENTH domain, with the transcription factor promyelocytic leukemia Zn^{2+} finger protein (PLZF). Leptomycin B, an antifungal antibiotic, which inhibits the Crm1-dependent nuclear export pathway, induces an accumulation of epsin 1 in the nucleus. These findings suggest that epsin 1 may function in a signaling pathway connecting the endocytic machinery to the regulation of nuclear function.

Key words: clathrin • Eps15 homology domain • catenin • karyopherin • endocytosis

Introduction

Epsin (Eps15 interactor)[1] proteins were recently identified as interacting partners for the EH (Eps15 homology) domains of Eps15 (Chen et al., 1998; Rosenthal et al., 1999). Both epsin 1 and 2 interact with components of the clathrin coat, partially localize at clathrin-coated pits, and are involved in clathrin-mediated endocytosis (Chen et al., 1998; Rosenthal et al., 1999). The NH$_2$-terminal 140 amino acids of epsin constitute a phylogenetically conserved module termed the ENTH domain (epsin NH$_2$-terminal homology domain; Kay et al., 1999), which is also found in proteins that are substantially different from epsin outside of this domain (Chen et al., 1998; Kay et al., 1999; Rosenthal et al., 1999). Epsin binding to Eps15 (Salcini et al., 1997), as well as to other EH domain-containing proteins (Kay et al., 1999; Hussain et al., 1999; Nakashima et al., 1999; Sengar et al., 1999), is mediated by asparagine-proline-phenylalanine (NPF) motifs, found in the COOH-terminal domain. The central region of epsin contains a clathrin binding consensus and multiple copies of the motif DPW/F typically found in proteins that interact with the α-adaptin subunit of the clathrin adaptor AP-2 (Owen et al., 1999; Traub et al., 1999). Accordingly, epsin binds via this region to both clathrin and AP-2 (Chen et al., 1998;

Table I. Crystallographic Data Collection Statistics

	Unique refl.	Redundancy	Completeness	I/σ	R$_{sym}$*
	n		*%*		*%*
SeMet λ$_1$ (1.06883 Å)	24057	5.44 (2.03)	93.6 (68.3)	25.3 (2.8)	5.6 (20.2)
SeMet λ$_2$ (0.97984 Å)	25278	5.82 (3.07)	98.4 (88.2)	20.5 (2.2)	7.1 (40.0)
SeMet λ$_3$ (0.97961Å)	25300	5.89 (3.05)	98.4 (89.0)	20.8 (2.3)	7.2 (40.5)
SeMet λ$_4$ (0.92526 Å)	25598	6.01 (3.83)	99.6 (97.1)	17.0 (1.9)	8.3 (57.2)

Values in parentheses are for the high resolution bin (1.86–1.80) Å.

*R$_{sym}$ = $\Sigma_h\Sigma_i|I_i(h) - \langle I(h)\rangle|/ \Sigma_h\Sigma_i I_i(h)$ where $I_i(h)$ is the i-th measurement and $\langle I(h)\rangle$ (is the mean of all measurements of I(h) for Miller indices h.

Rosenthal et al., 1999). Epsin 1 is very abundant in brain and probably participates in membrane recycling at the synapse (Chen et al., 1998).

Yeast homologues of epsin, Ent1p and Ent2p, were shown to be involved in endocytosis and actin function (Wendland et al., 1999). The NPF motifs of the Ent proteins bind the EH domains of Pan1, which shares functional similarities with Eps15 (Wendland et al., 1999). Based on genetic studies, the ENTH domain represents the functionally most important portion of the Ent proteins. Whereas a strain harboring a disruption of both the *ENT1* and *ENT2* genes is not viable, expression of the ENTH domain of either protein in this double mutant background, but not expression of Entp deletion mutants lacking this domain, was sufficient to rescue the lethal phenotype (Wendland et al., 1999).

So far, the function of the ENTH domain is unknown. To gain insight into its function, we have determined the X-ray crystal structure of the ENTH domain of rat epsin 1 and investigated its protein-binding properties. Our findings suggest an unexpected dual function of epsin in the cytoplasm and in the nucleus.

Materials and Methods

ENTH Expression for Structural Determination

ENTH of rat epsin 1 was expressed as an NH$_2$-terminal GST fusion using the pGEX-6-1 expression vector (Amersham Pharmacia Biotech). The plasmid was introduced into B834(DE3) cells (Novagen) and grown in defined M9 media supplemented with 50 mg/liter selenomethionine (SeMet; Leahy et al., 1994) and 0.1 mg/ml ampicillin. Cells were grown to an optical density of 2 measured at 600 nm, at which time the culture was induced using 0.8 mM isopropyl-β-D-thiogalactopyranoside and allowed to continue growing for ~4–5 h. Cells were harvested by centrifugation, flash frozen, and stored at −80°C. Protein purification was performed using 60 g of frozen cells resuspended in 200 ml of 50 mM Tris-HCL, pH 7.5, 200 mM NaCl, 10 mM DTT, and 2 mM PMSF, and were then homogenized by sonication. The cell lysate was pelleted by centrifugation at 46,000 *g* and 4°C for 50 min. The supernatant was added to 3 ml of glutathione

Sepharose 4B beads (Amersham Pharmacia Biotech). After gentle mixing for 1 h, GST-Sepharose beads containing bound ENTH were washed four times with 50 ml wash buffer (20 mM Tris-HCl, pH 7.5, 200 mM NaCl, and 10 mM DTT). GST-Sepharose beads with bound ENTH were then resuspended in 15 ml of wash buffer with ~100 μg bovine thrombin and incubated overnight with agitation. As a note, although pGEX6-1 is a rTEV cleavable GST fusion vector, we found that rTEV cleavage was not effective. However, thrombin cleaves quite well at an internal site 10 amino acids into the ENTH domain. Crystals of lesser quality have been obtained with rTEV cleaved protein, but this protein showed significant degradation in crystal trays, so studies with these crystals were not pursued. Cleaved ENTH protein was separated from glutathione-Sepharose beads and injected onto a Superdex 75 16/60 size-exclusion column (Amersham Pharmacia Biotech) at 0.5 ml/min in wash buffer. Fractions containing ENTH as determined by UV absorption and SDS-PAGE were pooled and dialyzed into 20 mM Na-Hepes, pH 7.5, 20 mM NaCl, and 10 mM DTT. ENTH was then concentrated to ~7.5 mg/ml (Millipore ultrafree spin concentrator), flash frozen in 100 μl aliquots using liquid nitrogen, and stored at −80°C.

Crystallization and Data Collection

Initial crystals were obtained by hanging drop vapor diffusion at 20°C. 1 μl of protein solution at ~7.5 mg/ml was mixed with 1 μl of mother liquor containing 100 mM Na-Hepes, pH 7.5, 10% polyethylene-glycol (PEG) 1000, and 8% ethylene glycol on a siliconized glass coverslip, and equilibrated against 0.5 ml of mother liquor. Crystals typically grew to full size (220 × 220 × 100 μm) in 30–40 h. Crystals were cryoprotected by sequential transfer into mother liquor containing 5% increasing increments of ethylene glycol to a final concentration of 30%. The crystals were then flash frozen in liquid nitrogen-cooled liquid propane that was subsequently frozen in liquid nitrogen. ENTH crystallized in space group P3$_1$21 with one molecule per asymmetric unit, and a solvent content of 40% as determined by the Matthews coefficient (Matthews, 1968). Diffraction data were collected at four wavelengths, and processed using DENZO/scalepack (Otwinowski and Minor, 1997; Table I).

Structure Determination

Four of the five expected selenium sites were located in an anomalous difference Patterson map calculated at the peak wavelength using an automated Patterson heavy-atom search method (Grosse-Kunstleve and Brunger, 1999) implemented in the Crystallography & NMR System (CNS; Brunger et al., 1998). The final site was located after initial multiwavelength anomalous dispersion (MAD) phasing with CNS using a log likelihood gradient map (Bricogne, 1997). The MAD phasing statistics were ex-

Table II. Crystallographic Phasing Statistics

	Overall isomorphous and dispersive differences*				Phasing power as defined in CNS‡	
Wavelength	λ$_1$	λ$_2$	λ$_3$	λ$_4$	F$^+$ Friedel mate	F$^-$ Friedel mate
λ$_1$ (remote)	0.0427	0.0766	0.0916	0.0569	(reference)	0.51
λ$_2$ (inflection)		0.0570	0.0484	0.0859	2.67	2.79
λ$_3$ (peak)			0.0707	0.0967	3.80	3.31
λ$_4$ (remote)				0.0843	0.69	1.06

*Values are $\langle(\Delta|F|)^2\rangle^{1/2}/\langle|F|^2\rangle^{1/2}$, where $\Delta|F|$ is the dispersive (off-diagonal element), or Bijvoet difference (diagonal elements), computed between 500 and 1.8 Å resolution.

‡MAD phasing power is defined as $[\langle| |F_{\lambda 1}^+|-|F_{\lambda i}^{(+/-)}| |^2\rangle/\int_\phi P(\phi)(\|F_{\lambda 1}^+|e^{i\phi}+\Delta F|-| F_{\lambda i}^{(+/-)}|)^2 d\phi]^{1/2}$ where $P(\phi)$ is the experimental phase probability distribution, i is any wavelength. F^+ and F^- correspond to a Bijvoet pair of structure factors. ΔF is the anomalous scatterer structure factor difference for a particular lack of closure expression.

Table III. Crystallographic Figure-of-Merit

Bragg Spacing Limits (Å)	Overall (43.14–1.79)	3.58	2.84	2.48	2.26	2.09	1.97	1.87	1.79
Figure-of-Merit (FOM)	0.72	0.92	0.91	0.85	0.77	0.69	0.58	0.46	0.33

MAD phasing power is defined as $[\langle||F_{\lambda 1}^+|-|F_{\lambda i}^{(+/-)}||^2\rangle/\int_\phi P(\phi)(||F_{\lambda 1}^+|e^{i\phi}+\Delta F|-|F_{\lambda i}^{(+/-)}|)^2 d\phi]^{1/2}$ where $P(\phi)$ is the experimental phase probability distribution, i is any wavelength. F^+ and F^- correspond to a Bijvoet pair of structure factors. ΔF is the anomalous scatterer structure factor difference for a particular lack of closure expression.

cellent (Table II). The phases were improved by density modification using solvent flipping (Abrahams and Leslie, 1996) and histogram matching (Zhang and Main, 1990; Table III). A representative region of the resulting electron density map is shown in Fig. 1. Nearly all side chains were clearly defined in the electron density map. All map and phasing calculations were carried out using CNS (Brunger et al., 1998).

Model Building and Refinement

An initial model was built with the program O (Jones et al., 1991), using the electron density map obtained by MAD phasing and subsequent density modification. All of the ENTH domain could be unambiguously traced except for residues 1–5, 20–23, 149, and 150. Model refinement was monitored using the free R value (Brunger, 1992) computed from a randomly omitted 10% of the observed diffraction data. Refinement was carried out using alternating rounds of simulated annealing, torsion angle molecular dynamics (Rice and Brunger, 1994), restrained B factor refinement (Hendrickson, 1985), and model rebuilding. Model refinement was accomplished in CNS using the MLHL target (Pannu and Read, 1998) against the diffraction data at the low-energy remote wavelength. Final model statistics are given in Table IV and were calculated using CNS (Brunger et al., 1998) and Denzo (Otwinowski and Minor, 1997). The final model contains residues 16–160 of the ENTH domain, 65 ordered water molecules, and 3 ethylene glycol molecules.

Yeast Two-hybrid Screen

The ENTH domain of rat epsin 1 (amino acids 1–160 of rat epsin 1; Chen et al., 1998) fused to the LexA DNA-binding domain was used as bait to screen a rat brain Matchmaker activation domain library in pGAD10 (CLONTECH Laboratories, Inc.). The bait was transformed along with the library in the L40 reporter yeast strain. Yeast colonies that survived on histidine− plates were also tested for activation of the *LacZ* gene. Prey plasmids positive for *LacZ* were retransformed in yeast. Clones that did not transactivate with the LexA DNA-binding vector alone, but interacted with the ENTH-LexA DNA-binding domain, were restriction mapped and sequenced. A pair of primers specific to pGAD10 vector: 5′ CAT TTC GAT GAT GAA GAT ACC CCA CCA AAC C 3′, 5′ GTG CAC GAT GCA CAG TTG AAG TGA ACT TGC 3′; were used for

PCR of the inserts that were subjected to restriction mapping and sequence analysis. The specificity of the interaction between rPLZFΔPOZ (see Results) with the ENTH domain was further confirmed by testing the interaction of rPLZFΔPOZ-LexA DNA-binding domain with ENTH-Gal4 activation domain in the yeast two-hybrid assay. Deletion mutants of rPLZFΔPOZ were generated by PCR amplification of the desired fragments, which were subcloned into the pGAD424 activation domain vector (CLONTECH Laboratories, Inc.).

Affinity Purification

For affinity-purification of rat brain proteins, the same ENTH domain used for crystallographic studies was coupled to UltraLink Biosupport Medium (Pierce Chemical Co.) according to the manufacturer's instructions. A Triton X-100 extract of a rat brain total homogenate (10 mg/ml) was incubated with immobilized ENTH domain at 4°C and the bound material was analyzed by SDS-PAGE and Western blotting. Wild-type and mutant GST-ENTH fusion proteins were used for affinity purifications from Triton X-100 extracts of cells transfected with flag epitope-tagged rPLZFΔPOZ or full-length human promyelocytic leukemia Zn^{2+} finger protein (PLZF) according to standard procedures (Nemoto et al., 1997).

Generation of Mutant ENTH Domains

The mutant ENTH domains were obtained using PCR-based site-directed mutagenesis (Chen et al., 1999). The sequences of these mutant ENTH domains were confirmed by standard double-strand sequencing.

Leptomycin B Incubations

Leptomycin B (10 ng/ml; kind gift of Dr. M. Yoshida; Kudo et al., 1999) was added to the culture medium 16 h after transfection and cells were incubated for additional 3.5 h before fixation. A full-length GFP-tagged rat epsin 1 clone was constructed as described (Rosenthal et al., 1999) and used in the leptomycin B studies.

Antibodies and Miscellaneous cDNAs

Rabbit polyclonal antibodies against human PLZF and epsin were previ-

Table IV. Crystallographic Refinement

Resolution range	Overall										
Resolution (Å)	500–1.8 Å	500–3.88	3.08	2.69	2.44	2.27	2.13	2.03	1.94	1.86	1.80
R-value*	20.6	20.8	20.4	21.3	18.1	20.7	20.1	20.2	20.5	23.6	25.2
R_{free}[‡]	22.5	22.5	22.0	22.3	19.0	22.8	23.4	23.0	24.2	27.4	24.6
Luzzati coordinate error	0.21 Å										
Cross-validated Luzzati coordinate error	0.23 Å										
Bond-length deviation	0.005 Å										
Bond-angle deviation	1.12°										
Improper angle deviation	0.68°										
Dihedrals	18.0°										
Average B-factor	20.9 Å²										
RMSD for bonded main chain atoms	1.87 Å²										
RMSD for bonded side chain atoms	3.32 Å²										
Minimum B-factor	7.46 Å²										
Maximum B-factor	62.3 Å²										
% Residues in core φ-ψ region	91.1										
% Residues in disallowed regions	0.0										

*R = $\Sigma(|F_{obs}|-k|F_{calc}|)/\Sigma|F_{obs}|$.
[‡]Free *R* value is the *R* value obtained for a test set of reflections, consisting of a randomly selected 10% subset of the diffraction data, not used during refinement.

ously described (Chen et al., 1998; Grignani et al., 1998). Rabbit polyclonal antibodies against rat PLZF were obtained using GST-rPLZFΔ POZ as the immunogen. The resulting serum was first depleted of anti-GST antibodies by incubation with GST beads and then affinity-purified with GST-rPLZFΔPOZ fusion protein. A cDNA encoding GFP-β-galactosidase fusion protein in pHM830 was a kind gift of Dr. T. Stamminger (Institute fur Klinische und Molekulare Uirologie, Universitat Erlangen-Nurnberg, Erlangen, Germany). Xpress-tagged epsin 1 cDNA was previously described (Chen et al., 1998). A human PLZF cDNA in pcDNA3 was a kind gift of Dr. P.G. Pelicci (European Institute of Oncology, Milano, Italy). The cDNA encoding GFP-rat epsin 1 was generated by subcloning the epsin 1 cDNA into the pEGFP-C1 vector (CLONTECH Laboratories, Inc.).

Miscellaneous Procedures

Cell transfection, immunoprecipitation, immunofluorescence, GST-fusion protein production, SDS-PAGE, Western blotting, and protein assay were carried out as previously described (Chen et al., 1998).

Results

Structure Determination

The ENTH domain of rat epsin 1 (residues 1–160) was expressed as a GST-fusion protein in *Escherichia coli*. After cleavage of the fusion protein and purification, crystals of the ENTH domain were obtained by hanging drop vapor diffusion in a polyethylene-glycol condition at 4°C. SeMet-substituted ENTH domain crystallized in a similar condition, and these crystals were used for further study. Diffraction data were collected for a MAD experiment (Hendrickson, 1991) using synchrotron radiation at four wavelengths around the selenium K absorption edge. Crystals belonged to space group $p3_121$, with unit cell parameters: $a = b = 49.81$ Å, $c = 99.97$ Å, $\alpha = \beta = 90°$, and $\gamma = 120°$. The crystals contained $\sim40\%$ solvent and diffracted to a minimum Bragg spacing of 1.8 Å. The electron density map obtained from density-modified MAD phases was superb, and easily traceable (Fig. 1). The final refined model has a free R value (Brunger, 1992) of 22.5% for all reflections with a Bragg spacing >1.8 Å.

General Features of the Structure

The ENTH domain forms a compact globular domain (Fig. 2, A and B) with a solvent accessible surface area of $\sim8,200$ Å. The structure is composed of eight α helices connected by loops of varying length. The general topology of the structure is determined by three helical hairpins ($\alpha1$–2, $\alpha3$–4, and $\alpha6$–7) that are stacked consecutively with a right-handed twist. This stacking gives the ENTH domain a rectangular appearance when viewed face on (Fig. 2, A i and B i). The two primary faces, one concave and one convex, are made up of parallel α helices (Fig. 2 A).
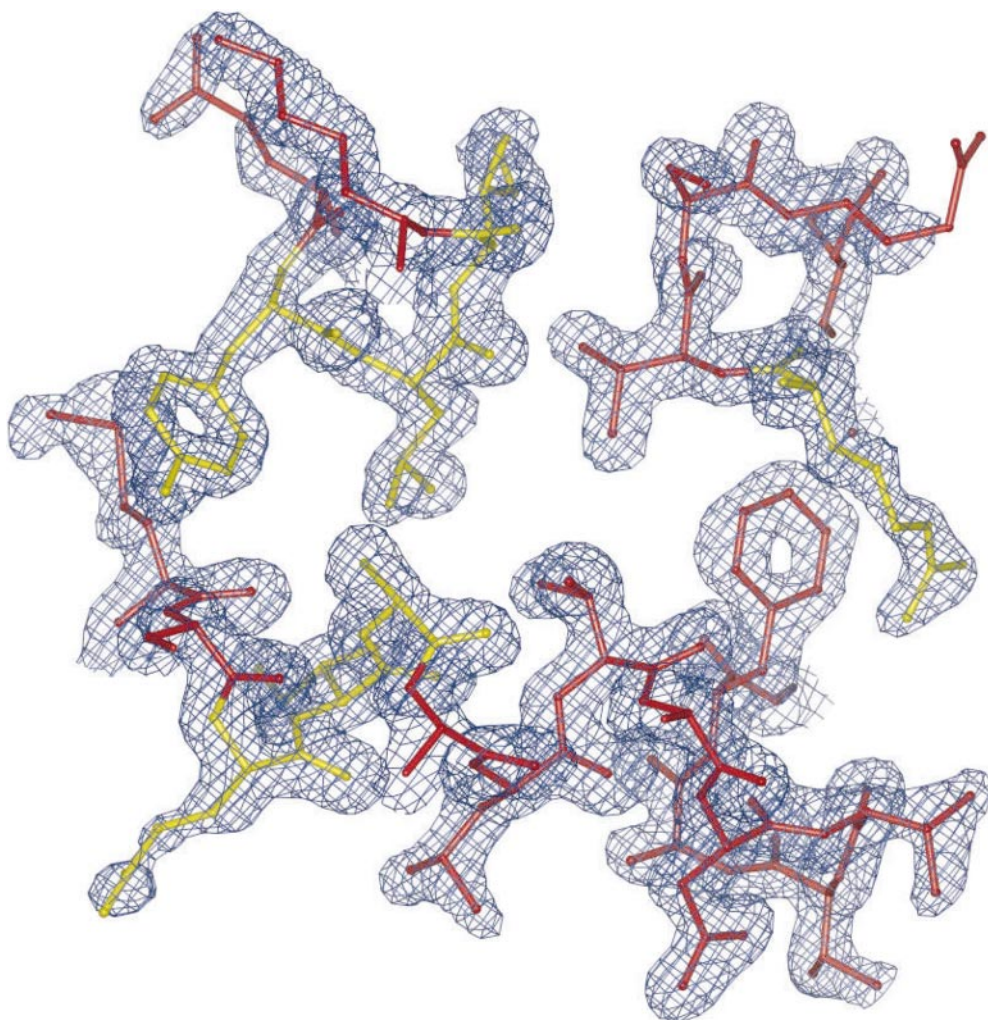

Figure 1. Representative experimental electron density map for residues 30–44, 72–76, and 81–85 contoured at 1.4 Å obtained by MAD phasing and subsequent density modification. The final refined model is shown using a ball and stick representation, with residues in yellow indicating a high degree of sequence conservation. The backbone trace was clearly visible for a portion of α helix 2, and exceptional density was found for most side chains. Figure generated using MOLSCRIPT (Kraulis, 1991).

Figure 2. Overall structure of the ENTH domain and sequence alignment. A, Ribbon drawings of the ENTH domain. The drawing at right (ii) is related to the drawing at left (i) by a 60° rotation towards the viewer. The eight α helices of the ENTH domain are indicated by different colors. The T28A, R72A, and G88S mutations made in this study are indicated by aquamarine balls. α Helices 1–8 are indicated in i. Figures generated using MOLSCRIPT (Kraulis, 1991). B, Sequence conservation projected onto accessible surface representations of the ENTH domain. These surface representations correspond to the same two views (i and ii) in A. Figures generated using GRASP (Nicholls, 1991). C, Sequence alignment of ENTH domains from various species. Identical residues are indicated in red, conserved residues in yellow. Green stars indicate residues that have been mutated in this study. The schematic diagram above the alignment indicates the location of loop and helix regions. Accession number and species as follows: epsin 1, AAC33823, *Rattus norvegicus*; epsin 2b, AAC78609, *Homo sapiens*; BAA11488, *Homo sapiens*; MP90, AAC-60123, *Xenopus laevis*; liquid facets, AAF05113, *Drosophila melanogaster*; Ent1, 6320039, *S. cerevisiae*; Ent2, 6323235, *S. cerevisiae*; 6322585, *S. cerevisiae*; AAC64305, *Arabidopsis thaliana*; CAA19587, *Schizosaccharomyces pombe*; AF-10, AAB68030, *Avena fatua*. Alignment generated using CLUSTAL W (Thompson et al., 1994) and AMAS (Livingston and Barton, 1993).
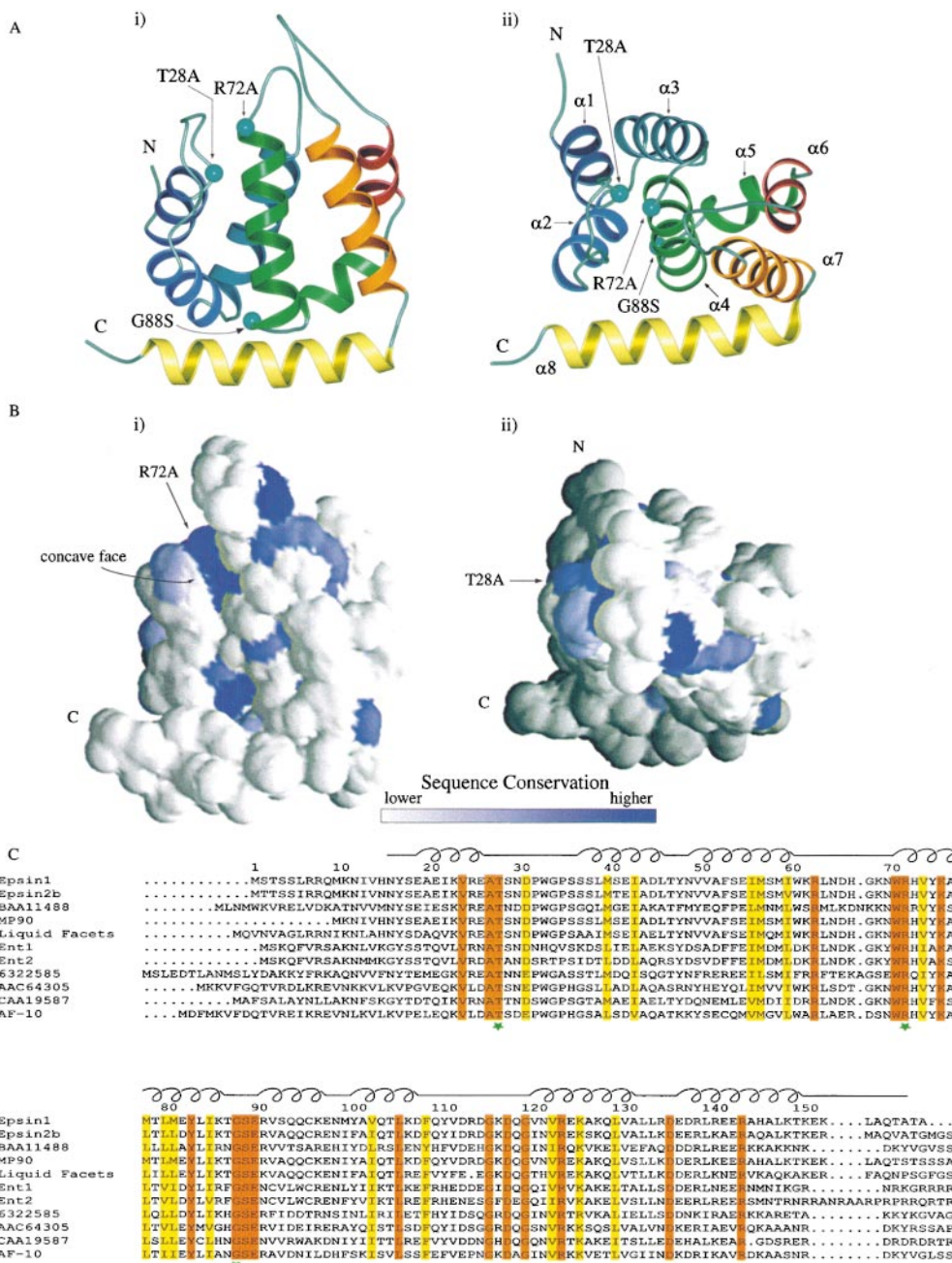
The COOH-terminal α helix (α8) folds back across the domain, framing the bottom edge perpendicular to the central hairpin (α3–4). From the opposite edge, loops that connect α helices 1–2, 3–4, and 6–7 form a conical projection, lending a wedge-like appearance (Fig. 2, A i).

The ENTH domain family contains several highly conserved residues (Chen et al., 1998; Kay et al., 1999; Rosenthal et al., 1999; Fig. 2 C). The most highly conserved residues fall roughly into two classes: internal residues that are involved in packing and therefore are necessary for structural integrity, and solvent accessible residues that may be involved in protein–protein interactions. Two large regions of high conservation emerge on the molecular surface: a larger patch formed primarily from residues on loop 2 and α helix α4, and a smaller patch was found near loop 7 (Fig. 2, A, B, and C).

Structural Alignment and Comparison

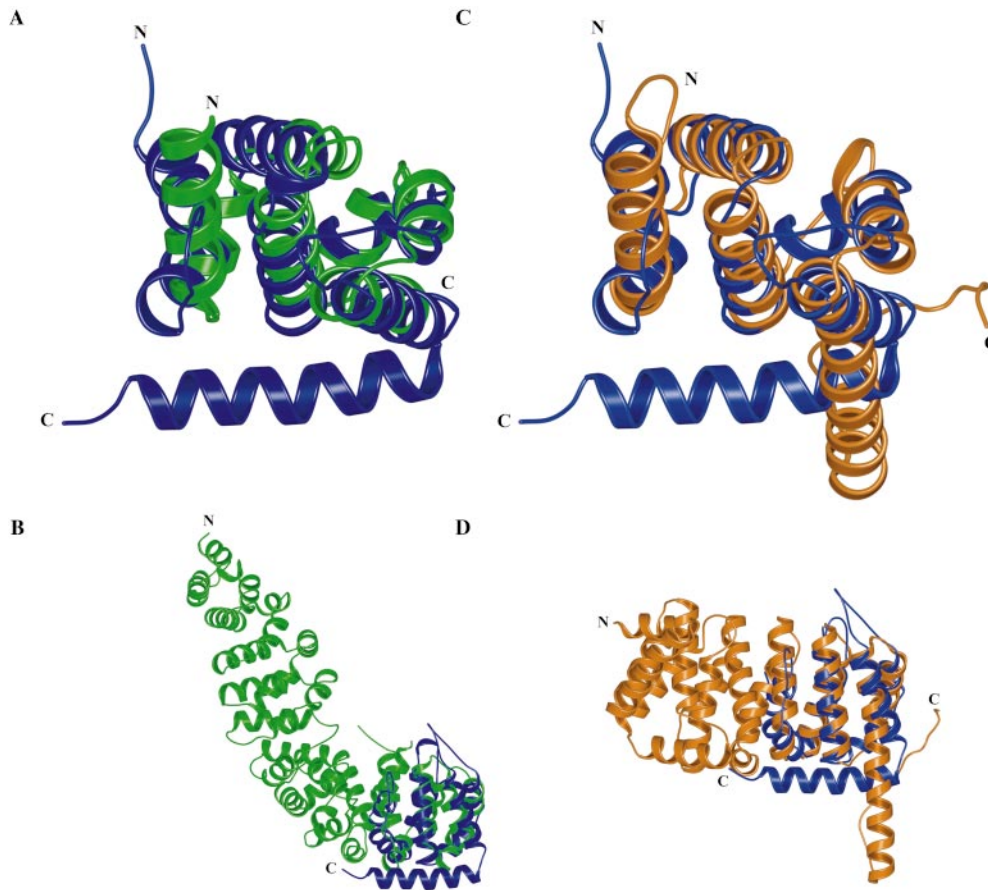A structural similarity search using DALI (Holm and

Figure 3. Alignment of structurally similar protein folds. A, Alignment of the ENTH domain of epsin 1 (blue) with one portion of the *armadillo* repeat region of β-catenin (green), showing a good overall superimposition between α helices in the central region of the domain. This alignment shows the ENTH domain in the same orientation as in Fig. 2, A ii. B, Same as A, but showing the entire β-catenin *armadillo* region and the ENTH domain in the same orientation as in Fig. 2, A i. C, Alignment of the ENTH domain (blue) with a segment of karyopherin-β (orange). This alignment shows the ENTH domain in the same orientation as in Fig. 2, A ii. D, Same as C, showing the entire structure of karyopherin-β and the ENTH domain in the orientation of Fig. 2, A i. Structural alignments produced using WHATIF (Vriend, 1990). Figures generated using MOLSCRIPT (Kraulis et al., 1991).

Sander, 1993) identified proteins that are structurally similar to ENTH, but not related by primary sequence. The ENTH structure is most similar to an *armadillo* repeat segment from β-catenin (Huber et al., 1997; Fig. 3, A and B), the HEAT repeat unit from karyopherin-β (importin-β; Chook and Blobel, 1999; Cingolini et al., 1999; Fig. 3, C and D), and to the scaffolding subunit of protein phosphatase 2A (Groves et al., 1999). Both *armadillo* and HEAT repeats are protein–protein interaction modules composed exclusively of α helices, and form structures with two primary faces, one concave and one convex. *armadillo* and HEAT repeats bind to target proteins with their concave face (Huber et al., 1997; Chook and Blobel, 1999; Cingolini et al., 1999; Groves et al., 1999). Structural superimposition of the ENTH domain with either type of repeat aligns their concave faces (Figs. 2 and 3), which contain the largest patch of conserved surface residues (Vriend, 1990). The C_α superposition of ENTH with karyopherin-β has a root mean square difference (RMSD) of 1.5 Å, whereas the C_α superposition with β-catenin produces an RMSD of 1.8 Å.

Isolation of an ENTH Domain Binding Protein, PLZF

The structural similarity of the ENTH domain to *armadillo* and HEAT repeats suggests that the ENTH domain may interact with other proteins. We searched for potential binding partners of the ENTH domain of rat epsin 1 (residues 1–160) using the yeast two-hybrid method. A bait construct consisting of the ENTH domain fused to the DNA-binding domain of LexA was used to screen a pGAD10 rat brain cDNA library. 20 of the clones isolated by the screen were all identical, and encoded an open reading frame highly homologous (96% identity) to the COOH-terminal portion of human PLZF (corresponding to amino acids 262–673 of the human protein). PLZF is a transcription factor containing an NH_2-terminal BTB/POZ domain and nine C_2H_2 Zn^{2+} finger motifs (Li et al., 1997; Fig. 4 A).

The identification of a transcription factor as an interaction partner for the ENTH domain of epsin 1 seemed surprising at first, given the known function of epsin 1 at the cell periphery. However, β-catenin family proteins, which contain a structurally related module, have a dual function in the cell cortex and in the nucleus (Barth et al., 1997; Willert and Nusse, 1998). Furthermore, catenin p120, which contains *armadillo* repeats, binds to a POZ/BTB-Zn^{2+} finger containing transcription factor, Kaiso, that is homologous to PLZF (Daniel and Reynolds, 1999). The interaction of catenin p120 with Kaiso is mediated by the *armadillo* repeat region of p120, and by the COOH-terminal portion of Kaiso, corresponding to the region of PLZF selected by the yeast two-hybrid screen. In addition, based on the binding properties of protein fragments, the Zn^{2+} finger region and upstream sequences of both Kaiso and PLZF are required for the interaction with catenin p120 and ENTH, respectively (Daniel and Reynolds, 1999; and Fig. 4 A). The similarity of these two interactions is likely

to reflect evolutionary conservation. We hypothesized that epsin and PLZF are physiological partners, and carried out further biochemical and functional studies to validate this interaction.

Biochemical Interaction of Epsin and PLZF

To verify the interaction of PLZF and epsin, affinity purification experiments were performed using immobilized ENTH domain. The GST-ENTH domain, but not GST alone, specifically retained a flag-tagged–rPLZFΔPOZ fragment (the protein fragment of PLZF lacking the POZ domain, corresponding to the fragment isolated by the yeast two-hybrid screen) from extract of transfected CHO cells (Fig. 4 B). In addition, purified GST-free ENTH domain conjugated to beads, but not beads alone, interacted with endogenous PLZF from a rat brain extract (Fig. 4 C).

To determine whether epsin and PLZF interact in vivo, immunoprecipitation experiments from rat brain extracts were carried out. Antiepsin antibody, but not control IgGs, coprecipitated PLZF, but not p53 (a negative control; Fig. 4 D). Conversely, anti-PLZF antibody, but not preimmune IgGs, coprecipitated epsin (Fig. 4 E), but not p53 (not shown). While epsin is present in the cytosol and further concentrated at the synapse, PLZF was shown to be primarily localized in the nucleus (Ruthardt et al., 1998). However, a cytosolic pool of PLZF was observed by immunofluorescence in brain (not shown).

To further assess the specificity of the binding of the ENTH domain to PLZF, highly conserved residues of the ENTH domain were altered by site directed mutagenesis: T28 to A, R72 to A, and G88 to S. Mutation of glycine at position 88 was previously found to confer temperature sensitivity to the function of yeast Ent1p (Wendland et al., 1999). Wild-type and mutant ENTH domains were expressed as GST fusion proteins and used to affinity purify flag-tagged human PLZF expressed in CHO cells. As shown by Fig. 4 F, wild-type, but not mutant ENTH domains, pulled down PLZF from transfected cell extracts. A control protein, clathrin, was not retained by any of these fusion proteins.

PLZF Can Recruit Epsin to the Nucleus

Based on immunofluorescence, most epsin is found in the cytosol, even after overexpression (Chen et al., 1998; Rosenthal et al., 1999; Fig. 5 A). The interaction of epsin 1 with PLZF raises the possibility that epsin may be found in the nucleus under certain conditions. Enhanced expression of PLZF may increase the fraction of epsin 1 localized in the nucleus and allow the visualization of a nuclear epsin pool by immunofluorescence. When either full-length human PLZF or rPLZFΔPOZ were overexpressed by transfection, both proteins partially accumulated in the nucleus (Fig. 5 A, and not shown). In cells cotransfected with epsin 1 and PLZF, a nuclear pool of epsin was also observed (the concentration of endogenous epsin is below detectability with our antibodies; Chen et al., 1998).

We next investigated whether epsin physiologically shuttles between the nucleus and the cytoplasm. The antifungal antibiotic, leptomycin B, was recently shown to block the Crm1-dependent nuclear export pathway and to induce a nuclear accumulation of several proteins which
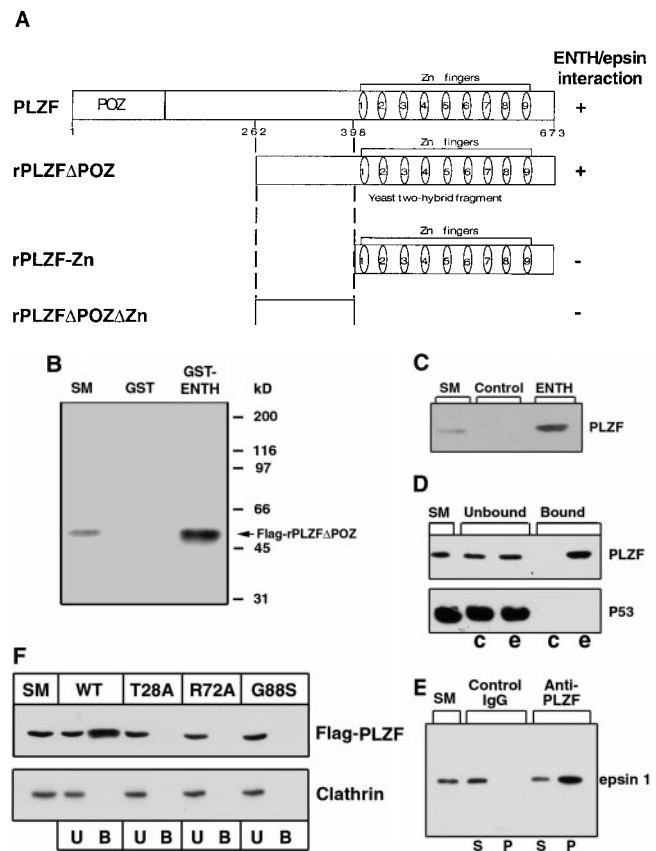

Figure 4. Interaction between the ENTH domain of epsin 1 and PLZF. A, Schematic representation of human PLZF and of the rat PLZF fragments discussed in this study. Numbers indicate amino acid numbers. B, Interaction of the GST-ENTH domain fusion protein with rPLZFΔPOZ. An extract of CHO cells transfected with flag-tagged rPLZFΔPOZ was affinity-purified on either GST or a GST-ENTH domain fusion protein. The starting material and the bead-bound material were analyzed by Western blotting using antibody directed against the flag epitope. C, ENTH domain affinity purification from a rat brain extract. A Triton X-100 extract of a rat brain total homogenate was affinity-purified on ENTH domain conjugated to beads or control beads. The starting material and the bead-bound material were analyzed by Western blotting for PLZF. D and E, PLZF and epsin can be coprecipitated from a rat brain Triton X-100 extract. D, Immuno-precipitates generated by antiepsin 1 antibodies or control IgGs were analyzed by Western blotting with anti-rat PLZF or anti-p53 (used as control) antibodies. E, Immunoprecipitates generated by anti-PLZF antibodies or control IgGs were analyzed by Western blotting using antiepsin 1 antibodies. F: Mutant ENTH domains fail to interact with PLZF. An extract of CHO cells transfected with flag-tagged human PLZF was affinity-purified on wild-type or mutant (T28A, R72A, and G88S) GST-ENTH domain fusion proteins. The starting material, the bead-unbound and the bead-bound material were analyzed by Western blotting using antibody directed against the flag epitope or anticlathrin antibody as a control. B, Bead-bound; c, control IgGs; e, antiepsin antibodies; P, pellet; S, supernatant; SM, starting material; U, bead-unbound.

shuttle between the nucleus and the cytoplasm (Nishi et al., 1994; Kudo et al., 1999; Van Hengel et al., 1999). We examined whether leptomycin B affected the intracellular distribution of epsin in CHO cells transiently transfected
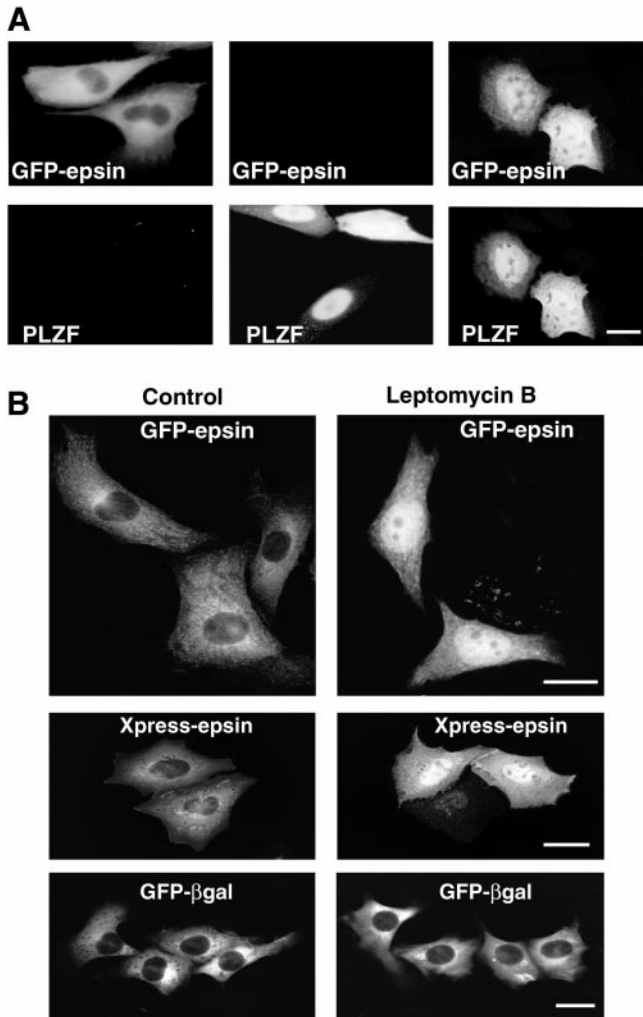
Figure 5. Immunofluorescence micrographs demonstrating that epsin may accumulate in the nucleus. A, Overexpression of human PLZF induces a partial accumulation of epsin in the nucleus. CHO cells were transiently transfected with epsin alone, human PLZF alone, or both proteins together, and then analyzed by confocal microscopy immunofluorescence. A pool of epsin is localized in the nucleus only in cells expressing both proteins. B, Leptomycin B induces an accumulation of epsin in the nucleus. CHO cells were transiently transfected with GFP-epsin, Xpress-tagged epsin, or the control protein GFP-β-galactosidase (GFP-βgal) and incubated for 3.5 h in the presence of leptomycin B before microscopic analysis. An accumulation of epsin is observed in the nucleus only in cells treated with leptomycin B. GFP-β-galactosidase was only cytosolic both in the presence and in the absence of leptomycin B. Bars, 12 μm.

with either GFP-epsin 1 or Xpress-tagged epsin 1. As shown by Fig. 5 B, both epsin 1 fusion proteins accumulated in the nucleus after incubation with leptomycin B, but not in control cells. A GFP–β-galactosidase fusion protein used as a control did not accumulate in the nucleus regardless of the presence of leptomycin B.

Discussion

The crystal structure of the ENTH domain of epsin 1 revealed a relationship to other well characterized protein modules that could not have been predicted by primary amino acid sequence analysis. The ENTH domain adopts a fold strikingly similar to that of *armadillo* and HEAT repeats, two domains found in β-catenin and karyopherin, respectively. Structural similarity often indicates functional similarity. Accordingly, we have identified properties of epsin suggesting that this similarity is functionally meaningful.

β-Catenin was first discovered as a component of a cytoskeletal scaffold underlying the plasma membrane and is thought to play an important role in the function of the cortical cytoskeleton (Tao et al., 1996; Bullions and Levine, 1998). β-Catenin was subsequently found to be part of a signaling pathway from the cell surface to the nucleus, the so-called Wnt signaling pathway. Activation of the pathway leads to decreased phosphorylation and degradation of β-catenin and to its accumulation in the nucleus, where it regulates transcription (Barth et al., 1997; Willert and Nusse, 1998; Peifer and Polakis, 2000). Mammalian epsin was identified as an accessory factor in clathrin-mediated endocytosis (Chen et al., 1998; Kay et al., 1999; Rosenthal et al., 1999) and its homologues in yeast, Ent1p and Ent2p, were implicated both in endocytosis and actin function (Wendland et al., 1999). The predominant pool of epsin is localized in the cytosol (Chen et al., 1998; Rosenthal et al., 1999). However, our present results demonstrate that epsin binds a transcription factor, PLZF, and that it can enter the nucleus. More specifically, the nuclear accumulation of epsin produced by leptomycin B demonstrates that epsin shuttles physiologically between the cytoplasm and the nucleus. Leptomycin B blocks the Crm1-dependent nucleocytosolic export pathway (Nishi et al., 1994; Kudo et al., 1999; Van Hengel et al., 1999), thus implying that nuclear accumulation of epsin results from an imbalance between nuclear import and nuclear export. An attractive possibility is that a regulated interaction of epsin with cytosolic components, possibly mediated by its phosphorylation (Chen et al., 1999), may control the nuclear pool of epsin and, via PLZF, the transcription of specific genes. This regulation may occur in response to external stimuli that activates endocytosis. This scenario defines a new regulatory pathway from the endocytic machinery to the nucleus.

These findings are convergent with recent studies of the epsin binding protein Eps15. As in the case of epsin, the role of Eps15 in clathrin-mediated endocytosis is well established and the bulk of Eps15 is localized in the cytosol (Salcini et al., 1997; Benmerah et al., 1998). However, an additional role of Eps15 in the regulation of nuclear functions has emerged. The same EH domain containing region of Eps15 that binds epsin also interacts with Numb and RAB/Hrb (Salcini et al., 1997). Numb binds Mdm2, a negative regulator of p53 (Juven-Gershon et al., 1998; Juven-Gershon and Oren, 1999), demonstrating a connection between Eps15 and a transcription factor. RAB/Hrb is a cofactor for export from the nucleus of the HIV protein Rev, and the EH domains of Eps15 cooperates with RAB/Hrb in the function of the Rev export pathway (Doria et al., 1999). This export pathway, in turn, is Crm1-dependent (Ullman et al., 1997). The role of Eps15 as a cofactor in nucleocytosolic export raises the possibility that even the similarity of the ENTH domain of epsin to the

karyopherins may reflect some functional relationship. The karyopherins are proteins implicated in cargo transport and recognition across the nuclear envelope via their HEAT repeat domains (Radu et al., 1995; Görlich, 1998; Pemberton et al., 1998; Nakielny and Dreyfuss, 1999).

Based on genetic studies, the ENTH domain is the most important functional domain of the yeast epsins, Ent1p and Ent2p (Wendland et al., 1999). Since the residues of the Ent proteins that interact with yeast EH domains and clathrin are localized outside the ENTH domain, the essential role of this domain may reflect its implication in nuclear functions. This possibility is consistent with our observation that at least one of the residues important for the function the ENTH domain of Ent1p is also required for the binding of rat epsin 1 ENTH domain to PLZF. Although an obvious orthologue of PLZF is not present in *Saccharomyces cerevisiae*, proteins with multiple Zn^{2+} finger motifs similar to those of PLZF are expressed by this organism. The similarity of PLZF to Kaiso, another transcription factor previously shown to bind the *armadillo* repeat region of catenin p120 (Daniel and Reynolds, 1999), indicates that the interaction of *armadillo*-repeat domains with this family of transcription factors is evolutionary conserved, and therefore likely to be physiologically important. The interaction of the ENTH domain with a transcription factor is not mutually exclusive with potential interactions with other proteins. Based on the property of the structurally related *armadillo* and HEAT repeats to bind multiple partners (Barth et al., 1997; Huber et al., 1997; Willert and Nusse, 1998; Chook and Blobel, 1999; Cingolini et al., 1999; Groves et al., 1999), it is likely that even the ENTH domain may have multiple physiological interactors. Pull-down experiments from rat brain have shown that tubulin, and to a lower extent coatomer (Rothman and Wieland, 1996), can bind ENTH domain of epsin 1 (our unpublished observations). However, the possible significance of these interactions remains unclear.

ENTH domains are present not only in proteins of the epsin family, but also in proteins which differ substantially from epsin outside this domain (Chen et al., 1998; Kay et al., 1999; Rosenthal et al., 1999). It is of interest that certain motifs are frequently found in such proteins. Besides NPF motifs that bind EH domains (Salcini et al., 1997), AP-2 and clathrin motifs, as well as FG motifs, are often present in them (Kay et al., 1999). FG repeats are signature motifs of nucleoporins (Radu et al., 1995), further emphasizing a potential connection of the ENTH domain to nuclear function. While epsin 1 does not contain FG repeats, most other epsin family members do (three or more such repeats are present in yeast Ent1 and Ent 2, in mammalian epsin 2, and in the epsin-like protein D79993.1). It is therefore possible that a dual function at the cell surface and in the nucleus may be a general property of most, possibly all, ENTH containing proteins.

Note Added in Proof. Mao et al. (Mao, Y., A. Nickitenko, X. Duan, T.E. Lloyd, N.N. Wu, H. Bellen, and F.A. Quiocho. 2000. *Cell.* 100:447–456) have recently reported the structure of VHS and FYVE tandem domains from the hepatocyte growth factor-regulated tyrosine kinase substrate. The VHS and ENTH domains align with an RMSD of ~1.8 Å, indicating an extremely similar fold. This is especially interesting because HRS is involved in membrane trafficking and signal transduction, perhaps indicating that this fold is a common motif in these areas.

References

Abrahams, J.P., and A.G.W. Leslie. 1996. Methods used in the structure determination of bovine mitochondrial F1 ATPase. *Acta Crystallogr.* D52:30–42.

Barth, A.I.M., I.S. Näthke, and W.J. Nelson. 1997. Cadherins, catenins and APC protein: interplay between cytoskeletal complexes and signalling pathways. *Curr. Opin. Cell Biol.* 9:683–690.

Benmerah, A., C. Lamaze, B. Bègue, S.L. Schmid, A. Dautry-Varsat, and N. Cerf-Bensussan. 1998. AP-2/Eps15 interaction is required for receptor mediated endocytosis. *J. Cell Biol.* 140:1055–1062.

Bricogne, G. 1997. Bayesian statistical viewpoint on structure determination: basic concepts and examples. *Methods Enzymol.* 276:361–423.

Brunger, A.T. 1992. Free R value: a novel statistical quantity for assessing the accuracy of crystal structures. *Nature.* 355:472–475.

Brunger, A.T., P.D. Adams, G.M. Clore, W.L. DeLano, P. Gros, R.W. Grosse-Kunstleve, J.S. Jiang, J. Kuszewski, M. Nilges, N.S. Pannu. 1998. Crystallography and NMR system: a new software suite for macromolecular structure determination. *Acta Crystallogr.* D54:905–921.

Bullions, L.C., and A.J. Levine. 1998. The role of beta-catenin in cell adhesion, signal transduction, and cancer. *Curr. Opin. Oncol.* 10:81–87.

Chen, H., S. Fre, V.I. Slepnev, M.R. Capua, K. Takei, M.H. Butler, P.P. Di Fiore, and P. DeCamilli. 1998. Epsin is an EH-domain–binding protein implicated in clathrin mediated endocytosis. *Nature.* 394:793–797.

Chen, H., V.I. Slepnev, P.P. DiFiore, and P. Decamilli. 1999. The interaction of epsin and eps15 with the clathrin adaptor AP-2 is inhibited by mitotic phosphorylation and enhanced by stimulation-dependent dephosphorylation in nerve terminals. *J. Biol. Chem.* 274:3257–3260.

Chook, Y.M., and G. Blobel. 1999. Structure of the nuclear transport complex karyopherin-β2-Ran·GppNHp. *Nature.* 399:230–237.

Cingolini, G., C. Petosa, K. Weis, and C.W. Müller. 1999. Structure of importin-α bound to the IBB domain of importin-β. *Nature.* 399:221–229.

Daniel, J.M., and A.B. Reynolds. 1999. The catenin p120^{ctn} interacts with Kaiso, a novel BTB/POZ domain zinc finger transcription factor. *Mol. Cell. Biol.* 19:3614–3623.

Doria, M., A.F. Salcini, E. Colombo, T.G. Parslow, P.G. Pelicci, and P.P. Di Fiore. 1999. The EH-based interaction between Eps15 and Hrb connects the molecular machinery of endocytosis to that of nucleocytosolic transport. *J. Cell Biol.* 147:1379–1384.

Görlich, D. 1998. Transport into and out of the cell nucleus. *EMBO (Eur. Mol. Biol. Organ.) J.* 17:2721–2727.

Grignani, F., S. De Matteis, C. Nervi, L. Tomassoni, V. Gelmetti, M. Cioce, M. Fanelli, M. Ruthardt, F.F. Ferrara, I. Zamir, et al. 1998. Fusion proteins of the retinoic acid receptor-α recruit histone deacetylase in promyelocytic leukaemia. *Nature.* 391:815–818.

Grosse-Kunstleve, R.W., and A.T. Brünger. 1999. A highly automated heavy-atom search procedure for macromolecular structures. *Acta Crystallogr.* D55:1568–1577.

Groves, M.R., N. Hanlon, P. Turowski, B.A. Hemmings, and D. Barford. 1999. The structure of the protein phosphatase 2A PR65/A subunit reveals the conformation of its 15 tandemly repeated HEAT motifs. *Cell.* 96:99–110.

Hendrickson, W.A. 1985. Stereochemically restrained refinement of macromolecular structures. *Methods Enzymol.* 115:252–270.

Hendrickson, W.A. 1991. Determination of macromolecular structures from anomalous diffraction of synchrotron radiation. *Science.* 254:51–58.

Holm, L., and C. Sander. 1993. Protein structure comparison by alignment of distance matrices (Dali 2.0). *J. Mol. Biol.* 233:123–138.

Huber, H.H., W.J. Nelson, and W.I. Weis. 1997. Three-dimensional structure of the armadillo repeat region of β-catenin. *Cell.* 90:871–882.

Hussain, N.K., M. Yamabhai, A.R. Ramjaun, A.M. Guy, D. Baranes, J.P. O'Bryan, C.J. Der, B.K. Kay, and P.S. McPherson. 1999. Splice variants of intersectin are components of the endocytic machinery in neurons and non-neuronal cells. *J. Biol. Chem.* 274:15671–15677.

Jones, T.A., J.Y. Zou, S.W. Cowan, and M.O. Kjeldgaard. 1991. Improved methods for building protein models in electron density maps and the location of errors in these models. *Acta Crystallogr.* A47:110–119.

Juven-Gershon, T., and M. Oren. 1999. Mdm2: the ups and downs. *Mol. Med.* 5:71–83.

Juven-Gershon, T., O. Shifman, T. Unger, A. Elkes, Y. Haupt, and M. Oren. 1998. The Mdm2 oncoprotein interacts with the cell fate regulator Numb. *Mol. Cell. Biol.* 18:3974–3982.

Kay, B.K., M. Yamabhai, B. Wendland, and S.D. Emr. 1999. Identification of a novel domain shared by putative components of the endocytic and cytoskeletal machinery. *Protein Science.* 8:435–438.

Kraulis, P.J. 1991. MOLSCRIPT: a program to produce both detailed and schematic plots of protein structures. *J. Appl. Cryst.* 24:946–950.

Kudo, N., M. Matsumori, H. Taoka, D. Fujiwara, E. Schreiner, B. Wolff, M. Yoshida, and S. Horinouchi. 1999. Leptomycin B inactivates CRM1/exportin 1 by covalent modification at a cysteine residue in the central conserved region. *Proc. Natl. Acad. Sci. USA.* 96:9112–9117.

Leahy, D.J., H.P. Erickson, I. Aukhil, P. Joshi, and W.A. Hendrickson. 1994. Crystallization of a fragment of human fibronectin: introduction of methionine by site-directed mutagenesis to allow phasing via selenomethionine. *Proteins.* 19:48–54.

Li, J.Y., M.A. English, H.J. Ball, P.L. Yeyati, S. Waxman, and J.D. Licht. 1997. Sequence-specific binding and transcriptional regulation by the promyelocytic leukaemia zinc finger protein. *J. Biol. Chem.* 272:22447–22455.

Livingston, C.D., and G.J. Barton. 1993. Protein sequence alignments: a strategy for the hierarchical analysis of residue conservation. *CABIOS.* 9:745–756.

Matthews, B.W. 1968. Solvent content of protein crystals. *J. Mol. Biol.* 33:491–497.

Nakashima, S., K. Morinaka, S. Kayoma, M. Ikeda, M. Kishida, K. Okawa, A. Iwamatsu, S. Kishida, and A. Kikuchi. 1999. Small G protein Ral and its downstream molecules regulate endocytosis of EGF and insulin receptors. *EMBO (Eur. Mol. Biol. Organ.) J.* 18:3629–3642.

Nakielny, S., and G. Dreyfuss. 1999. Transport of proteins and RNAs in and out of the nucleus. *Cell.* 99:677–690.

Nemoto, Y., M. Arribas, C. Haffner, and P. DeCamilli. 1997. Synaptojanin 2, a novel synaptojanin isoform with a distinct targetting domain and expression pattern. *J. Biol. Chem.* 272:30817–30821.

Nicholls, A., K. Sharp, and B. Honig. 1991. Protein folding and association: insights from the interfacial and thermodynamic properties of hydrocarbons. *Proteins.* 11:281–296.

Nishi, K., M. Yoshida, D. Fujiwara, M. Nishikawa, S. Horinouchi, and T. Beppu. 1994. Leptomycin B targets a regulatory cascade of crm1, a fission yeast nuclear protein, involved in control of higher order chromosome structure and gene expression. *J. Biol. Chem.* 269:6320–6324.

Otwinowski, Z., and W. Minor. 1997. Processing of x-ray diffraction data collected in oscillation mode. *Methods Enzymol.* 276:307–326.

Owen, D.J., Y. Vallis, M.E.M. Noble, J.B. Hunter, T.R. Dafforn, P.R. Evans, and H.T. McMahon. 1999. A structural explanation for the binding of multile ligands by the α-adaptin appendage domain. *Cell.* 97:805–815.

Pannu, N.S., and R.J. Read. 1998. Incorporation of prior phase information strengthens maximum likelihood structural refinement. *Acta Crystallogr.* D54:1285–1294.

Pemberton, L.F., G. Blobel, and J.S. Rosenblum. 1998. Transport routes through the nuclear pore complex. *Curr. Opin. Cell Biol.* 10:392–399.

Peifer, M., and P. Polakis. 2000. Wnt signaling in oncogenesis and embryogenesis: a look outside the nucleus. *Science.* 287:1606–1609.

Radu, A., M.S. Moore, and G. Blobel. 1995. The peptide repeat domain of nucleoporin Nup98 functions as a docking site in transport across the nuclear pore complex. *Cell.* 81:215–222.

Rice, L.R., and A.T. Brünger. 1994. Torsion angle dynamics: reduced variable conformational sampling enhances crystallographic structure refinement. *Proteins.* 19:277–290.

Rosenthal, J.A., H. Chen, V.I. Slepnev, L. Pellegrini, A.E. Salcini, P.P. Di Fiore, and P. De Camilli. 1999. The epsins define a family of proteins that interact with components of the clathrin coat and contain a new protein module. *J. Biol. Chem.* 234:33959–33965.

Rothman, J.E., and F.T. Wieland. 1996. Protein sorting by transport vesicles. *Science.* 272:227–234.

Ruthardt, M., A. Orleth, L. Tomassoni, E. Puccetti, D. Riganelli, M. Alcalay, R. Mannucci, I. Nicoletti, F. Grignani, M. Fagioli, and P.G. Pelicci. 1998. The acute promyelocytic leukaemia specific PML and PZL proteins localize to adjacent and functionally distinct nuclear bodies. *Oncogene.* 16:1945–1953.

Salcini, E.A., S. Confalonieri, M. Doria, E. Santolini, E. Tassi, O. Minenkova, G. Cesareni, P.G. Pelicci, and P.P. DiFiore. 1997. Binding specificity and in vivo targets of the EH domain, a novel protein–protein interaction module. *Genes Devel.* 11:2239–2249.

Sengar, A.S., W. Wang, J. Bishay, S. Cohen, and S.E. Egan. 1999. The EH and SH3 domain Ese proteins regulate endocytosis by linking to dynamin and Eps15. *EMBO (Eur. Mol. Biol. Organ.) J.* 18:1159–1171.

Tao, Y.S., R.A. Edwards, B. Tubb, S. Wang, J. Bryan, and P.D. McCrea. 1996. β-Catenin associates with the actin-bundling protein fascin in a noncadherin complex. *J. Cell Biol.* 134:1271–1281.

Thompson, J.D., D.G. Higgins, and T.J. Gibson. 1994. CLUSTAL W: improving the sensitivity of progressive multiple sequence alignment through sequence weighting, position-specific gap penalties and weight matrix choice. *Nucleic Acids Res.* 22:4673–4680.

Traub, L.M., M.A. Downs, J.L. Westrich, and D.H. Fremont. 1999. Crystal structure of the α appendage of AP-2 reveals a recruitment platform for clathrin-coat assembly. *Proc. Natl. Acad. Sci. USA.* 96:8907–8912.

Ullman, K.S., M.A. Powers, and D.J. Forbes. 1997. Nuclear export receptors from importin to exportin. *Cell.* 90:967–970.

Van Hengel, J., P. Vanhoenacker, K. Staes, and F. Van Roy. 1999. Nuclear localization of the p120ctn armadillo-like catenin is counteracted by nuclear export signal and E-cadherin expression *Proc. Natl. Acad. Sci. USA.* 96:7980–7985.

Vriend, G. 1990. WHAT IF: a molecular modeling and drug design program. *J. Mol. Graph.* 8:52–56.

Wendland, B., K.E. Steece, and S.D. Emr. 1999. Yeast epsins contain an essential N-terminal ENTH domain, bind clathrin and are required for endocytosis. *EMBO (Eur. Mol. Biol. Organ.) J.* 18:4383–4393.

Willert, K., and R. Nusse. 1998. β-catenin: a key mediator of Wnt signalling. *Curr. Opin. Genes Dev.* 8:95–102.

Zhang, K.Y.J., and P. Main. 1990. Histogram matching as a new density modification technique for phase refinement and extension of protein molecules. *Acta Crystallogr.* A46:41–46.